Available online at www.sciencedirect.com
SCIENCE DIRECT®
International Journal of Heat and Fluid Flow 24 (2003) 114–121
International Journal of HEAT AND FLUID FLOW
www.elsevier.com/locate/ijhff

Method to model dryer fabrics in paper machine scale using small-scale simulations and porous media model

Kati Laakkonen *

Process Flow Ltd Oy, Puolalanpuisto 1b A 21, 20100 Turku, Finland

Received 8 January 2001; accepted 15 June 2002

Abstract

This paper presents a method which has been developed in order to model dryer fabrics in a paper machine scale CFD model. The proposed method is based on source terms in the momentum equations of a large-scale model (porous media model). The coefficients for source terms are determined according to results of small-scale simulations of a periodic unit of a fabric. Additionally, the k–ε turbulence model has been modified in the large-scale model. A test for a dryer fabric is presented, and large-scale results are compared to wind tunnel measurements. The results show consistent behavior of the model.
© 2002 Elsevier Science Inc. All rights reserved.

Keywords: Porous media; Rough surfaces; Transpiration; Fabric

1. Introduction

The increase of paper machine speed has made air flow and pressure distribution in paper machine drying sections an important research area. Using CFD in the development process as a research tool has gained credibility lately.

It is known by experimental results (Fagerholm, 1990) that dryer fabrics have a significant effect on pressure levels in the drying section. Unfortunately, there has been no way to distinguish different fabrics in standard CFD models. An industrial R&D process requires a robust and reasonably accurate method to estimate fabric characteristics in a large-scale computational model. This article presents details of a model that is proposed. More results and background can be found in Laakkonen et al. (2001).

A dryer fabric is woven from monofilaments and the fabric affects the flow field around it because its surface is rough and it is permeable. Both characteristics are caused by the fabric structure. Roughness is due to the pattern of the fabric outer layer, whereas permeability is more governed by the structure of the inner part of a fabric. The monofilaments themselves are smooth and impermeable.

A fabric moving in a paper machine drags air with it due to friction and fabric roughness increases the magnitude of this phenomenon. The boundary layer on a fabric, when stopped by obstacles in a paper machine, causes overpressure and airflow through the permeable fabric, which in turn can cause detachment of paper from the fabric. Therefore a CFD model must include both roughness and permeability effects. This study does not consider any effects of temperature and moisture changes, which are present in the drying section. All simulations are isothermal.

The effect of roughness on a boundary layer is widely studied (for example: Antonia and Djenidi, 1997; Krogstad, 1991; Hellsten and Laine, 1998) but permeability gives way to transpiration through the fabric which also affects the boundary layer. There is no standard model to include both effects within wall functions of the program used.

The idea to simulate the flow field in a small periodic piece of rough surface or porous media has been used by Nakayama and Kuwahara (1999) and Mohammadi et al. (1998), for example. The method of transferring the information from the small-scale simulation to the large-scale model varies. In this article one possible method is proposed. All simulations have been carried out with

* Tel.: +358-2275-9583; fax: +358-2275-9580.
E-mail address: kati@processflow.fi (K. Laakkonen).

0142-727X/02/$ - see front matter © 2002 Elsevier Science Inc. All rights reserved.
PII: S0142-727X(02)00192-3

Nomenclature

A_{tot}	area of fabric unit
A_{free}	free area between fabric threads
A_j	face area of computational cell
A_ε, A_μ	constants of the near-wall turbulence model
C_{ij}	coefficient for inertial term of porous media model
C_μ, $C_{1\varepsilon}$, $C_{2\varepsilon}$	constants of the k–ε turbulence model
c_l	constant of the near-wall turbulence model
D_{ij}	coefficient for Darcian term of porous media model
F_i	forces in Cartesian directions x, y, z on fabric surface
f_i	forces per volume in Cartesian directions x, y, z
G_k	production of turbulent kinetic energy
k	turbulent kinetic energy
L	length scale for Reynolds number
l_ε, l_μ	length scales of the near-wall turbulence model
m	index used for slices of fabric
p	pressure
Re_y	Reynolds number of the near-fabric turbulence model
U_i	velocity components U, V, W in Cartesian directions: x, y, z
u_i'	fluctuating velocity components u', v', w' in Cartesian directions: x, y, z
x_i	Cartesian coordinates x, y, z
y	distance from the nearest wall in the near-wall turbulence model
ϕ	general variable
ε	dissipation of turbulent kinetic energy
κ	von Karman's constant
μ_{mol}	dynamic molecular viscosity
μ_t	dynamic turbulent viscosity
μ_e	dynamic effective viscosity
ν	kinematic viscosity
ρ	density
σ_ε, σ_k	turbulent Prandtl numbers of the k–ε turbulence model

Fluent 5, versions 5.0–5.4 (Fluent Incorporated, 1998) using unstructured meshes. The proposed large-scale fabric model consists of source terms in the momentum equations and manipulation of the turbulence model. The large-scale model results are compared to hot-wire measurements of wind tunnel tests.

2. Large-scale fabric model

2.1. Governing equations of the large-scale model

The flow in the large-scale simulations is assumed incompressible and turbulent, and the fluid is air (density $\rho = 1.225$ kg/m^3 dynamic molecular viscosity $\mu_{mol} = 1.789 \times 10^{-5}$ kg/ms). Turbulence is treated with Reynolds decomposition and the k–ε turbulence model. Thus mean flow equations can be expressed with the continuity equation for quasisteady flow

$$\frac{\partial U_i}{\partial x_i} = 0 \tag{1}$$

where U_i are mean velocity components in Cartesian coordinates x_i, and with the Reynolds-averaged Navier–Stokes equations for incompressible, quasisteady flow

$$\rho U_j \frac{\partial U_i}{\partial x_j} = -\frac{\partial}{\partial x_i}\left(p + \frac{2}{3}\rho k\right) + \frac{\partial}{\partial x_j}\left[\mu_{eff}\left(\frac{\partial U_i}{\partial x_j} + \frac{\partial U_j}{\partial x_i}\right)\right] + f_i \tag{2}$$

where p is static pressure, μ_{eff} is effective viscosity and k is turbulent kinetic energy. f_i is a source term caused by fabric effects. This source term is applied in a rectangular volume with the actual fabric thickness and the area of the actual fabric sheet. Effective viscosity is defined as

$$\mu_{eff} = \mu_{mol} + \mu_t \tag{3}$$

where μ_t is turbulent viscosity.

The transport equations of turbulent kinetic energy k and its dissipation rate ε are

$$\rho U_i \frac{\partial k}{\partial x_i} = \frac{\partial}{\partial x_i}\left[\left(\mu_{mol} + \frac{\mu_t}{\sigma_k}\right)\frac{\partial k}{\partial x_i}\right] + G_k - \rho\varepsilon \tag{4}$$

$$\rho U_i \frac{\partial \varepsilon}{\partial x_i} = \frac{\partial}{\partial x_i}\left[\left(\mu_{mol} + \frac{\mu_t}{\sigma_\varepsilon}\right)\frac{\partial \varepsilon}{\partial x_i}\right] + C_{1\varepsilon}\frac{\varepsilon}{k}G_k - C_{2\varepsilon}\rho\frac{\varepsilon^2}{k} \tag{5}$$

where G_k represents the generation of turbulent kinetic energy, calculated by equation

$$G_k = \mu_t\left(\frac{\partial U_i}{\partial x_j} + \frac{\partial U_j}{\partial x_i}\right)\frac{\partial U_j}{\partial x_i} \tag{6}$$

and $C_{1\varepsilon}$ and $C_{2\varepsilon}$ are constants. σ_ε and σ_k are turbulent Prandtl numbers for k and ε, respectively. Turbulent viscosity is calculated by

$$\mu_t = \rho C_\mu \frac{k^2}{\varepsilon} \tag{7}$$

where C_μ is a constant. The model constants have following values:

$$C_{1\varepsilon} = 1.44 \quad C_{2\varepsilon} = 1.92 \quad C_\mu = 0.09 \quad \sigma_\varepsilon = 1.3 \quad \sigma_k = 1.0$$

The near-wall areas are resolved with Fluent's two-layer zonal model (based on Wolfstein's model). The two-layer zonal model uses an algebraic equation for dissipation in the viscosity affected region of a boundary layer. The turbulent kinetic energy equation is solved in the same way as in the core region of the flow.

The value of the dissipation of turbulent kinetic energy ε is calculated by equation

$$\varepsilon = \frac{k^{3/2}}{l_\varepsilon} \tag{8}$$

Turbulent viscosity μ_t is calculated by equation

$$\mu_t = \rho C_\mu k^{1/2} l_\mu \tag{9}$$

Length scales l_ε and l_μ are obtained using equations

$$l_\mu = c_l y\left(1 - e^{-Re_y/A_\mu}\right) \tag{10}$$

$$l_\varepsilon = c_l y\left(1 - e^{-Re_y/A_\varepsilon}\right) \tag{11}$$

$$Re_y = \frac{\rho k^{1/2} y}{\mu_{\text{mol}}} \tag{12}$$

where y is the distance to the nearest wall and the constants have values

$$c_l = \kappa C_\mu^{-3/4} = 0.42 \times 0.09^{-3/4} = 2.556$$
$$A_\mu = 70$$
$$A_\varepsilon = 2c_l = 5.112$$

The model is applied in the vicinity of a wall where $Re_y < 200$.

The turbulence model for fabric simulations is modified only by changing the value of y in Eqs. (10)–(12). A length scale is calculated from the fabric geometry, as explained in Section 2.3, and used in the fabric volume and its vicinity. This forces the code to use the one-equation model in this area. As in the standard two-layer zonal model, the choice between one-equation model and full k–ε model is made according to value of Re_y.

2.2. Source terms in momentum equations

As a woven material, fabrics have periodical structures but the structure is far from homogenous. The geometry of a test fabric, standard style commercial dryer fabric Aeroplane 6028/515 of Albany International, is shown in Fig. 1. This modern dryer fabric has a rather smooth surface. However, the outer layers on both sides of the fabric have quite large void areas, while in inner parts of the fabric the void fraction is small. Thus, determining a typical pore size is somewhat difficult. The speed at which a fabric moves in a paper machine is known (relative speed between air and fabric), but simulations show that the relative speed in the fabric voids is always lower than the speed of the fabric. Therefore determining a typical Reynolds number (UL/ν, where U is relative speed of air, L is typical pore size and ν is the kinematic viscosity of air) of the flow becomes uncertain. However, with $U = 15$ m/s, $L = 1$ mm and $\nu = 1.46 \times 10^{-5}$ m^2/s, Reynolds number in the outer layer of a fabric is about 1000, which indicates non-Darcian flow. Thus, according to Fand et al. (1987) the fabric resistance to the flow should be modeled with

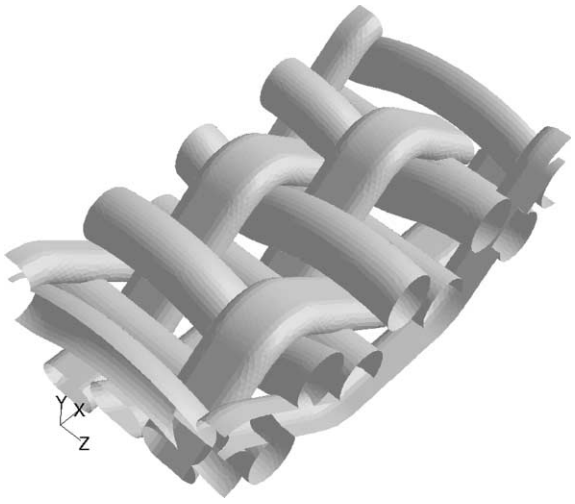

Fig. 1. Test fabric, standard style dryer fabric 6028/515. The thickness of the fabric is 1.3 mm. The width and length of the periodic unit are 2.3 and 4.0 mm, respectively.

$$\frac{\partial p}{\partial x} = DU + CU^2 \tag{13}$$

where D and C are constants, x is the direction of the flow and U is the mean velocity in this direction. The direction convention used in this study is x: main flow direction (machine direction in a paper machine), y: direction normal to fabric, and z: cross-direction.

In a porous media model, the resistance is given as a source term (force per volume) to the Reynolds averaged momentum equations, Eq. (2). The form of the source terms in the large-scale model is given by

$$\begin{pmatrix} f_x \\ f_y \\ f_z \end{pmatrix} = \begin{pmatrix} D_{11} & D_{12} & D_{13} \\ D_{21} & D_{22} & D_{23} \\ D_{31} & D_{32} & D_{33} \end{pmatrix} \begin{pmatrix} U \\ V \\ W \end{pmatrix} + \begin{pmatrix} C_{11} & C_{12} & C_{13} \\ C_{21} & C_{22} & C_{23} \\ C_{31} & C_{32} & C_{33} \end{pmatrix} \begin{pmatrix} |U|U \\ |V|V \\ |W|W \end{pmatrix} \tag{14}$$

This form was adopted from Fluent manuals (Fluent Incorporated, 1998). The Darcian term (first term on the right hand side of Eq. (14)) is defined as a function of viscosity, and the inertial term (second term on the right hand side of Eq. (14)) as a function of density. In this study the fluid is always air at constant density and

viscosity, and material property values are included in the coefficients C_{ij} and D_{ij}.

Normally the inertial term of Eq. (14) is expressed by (Nakayama and Kuwahara, 1999, for example)

$$\begin{pmatrix} f_x^{\text{inertial}} \\ f_y^{\text{inertial}} \\ f_z^{\text{inertial}} \end{pmatrix} = \begin{pmatrix} C_{11} & C_{12} & C_{13} \\ C_{21} & C_{22} & C_{23} \\ C_{31} & C_{32} & C_{33} \end{pmatrix} \begin{pmatrix} \sqrt{U^2+V^2+W^2}U \\ \sqrt{U^2+V^2+W^2}V \\ \sqrt{U^2+V^2+W^2}W \end{pmatrix} \tag{15}$$

A model according to Eq. (15) was tested also for this study, but the results were poor. Details are reported in Section 2.3.

The inhomogeneity of the fabric implies that C_{ij} and D_{ij} are not constants, but functions of position in the fabric, $D_{ij}(y)$ and $C_{ij}(y)$. In the test case of this study the non-diagonal terms have been left out, although this kind of simplification may not be justified for all types of fabric. The reason for leaving out the non-diagonal terms out was that they seemed to be small compared to the diagonal terms.

$D_{ij}(y)$ and $C_{ij}(y)$ can be determined from small-scale simulations. The information needed is average fluid velocity and forces acting on the fabric surface. In order to find the distribution of forces in the y-direction, the fabric surface has been divided into several parts (slices) by planes of constant y, and forces have been computed on these partial surfaces. The forces can be computed using a postprocessing function in the simulation program. Corresponding average velocities have been computed on planes located in the middle of the slices. An example of one slice and corresponding plane is shown in Fig. 2.

To find values corresponding to the source terms in the large-scale model, force components have been treated as follows:

$$f_i^m = \frac{F_i^m}{V_m} \tag{16}$$

$$V_m = A_{\text{tot}} \cdot h_m \tag{17}$$

where m is slice index, A_{tot} is total area of the fabric unit piece and h_m is the thickness of slice (difference of limiting y-values). F_i^m is the force on the fabric slice surface.

The area-weighted average of a flow variable ϕ on a plane m is computed as follows:

$$\phi_{ave}^m = \frac{1}{A_{\text{free}}^m} \sum_{j=1}^{n} \phi_j A_j \tag{18}$$

$$A_{\text{free}}^m = \sum_{j=1}^{n} A_j \tag{19}$$

where A_j is the area of a computational cell j, ϕ_j is the value of ϕ in cell j and A_{free} is the free area between the threads of the fabric on plane m.

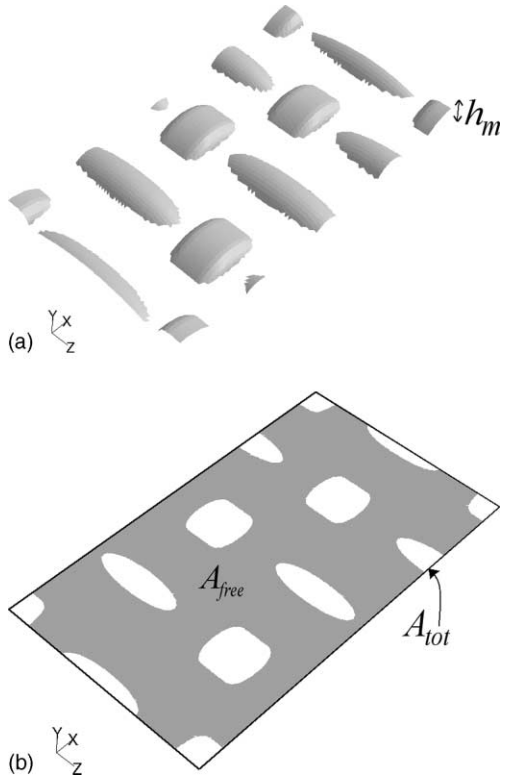

Fig. 2. One slice of the test fabric. (a) The fabric surface where forces are computed. (b) The plane on which average velocities are computed. A_{free} is the gray area, A_{tot} is the rectancular area marked with black lines.

The area-weighted averages are then handled as follows:

$$\phi^{*m} = \frac{A_{\text{free}}^m}{A_{\text{tot}}} \phi_{\text{ave}}^m + \frac{A_{\text{tot}} - A_{\text{free}}^m}{A_{\text{tot}}} \phi_{\text{f}} \tag{20}$$

where ϕ_{f} is the value in the fabric threads, that is in solid fraction of A_{tot}. If the fabric does not move in the small-scale simulations, the latter part of the sum is zero for velocity components. This averaging method is similar to superficial volume averaging in Quintard and Whitaker (2000). The only reason for using area-weighted averages instead of volume averages is that the previous is practically easier in the code used.

The coefficients D_i and C_i for each slice can then be solved from

$$f_i^m = D_i^m U_i^{*m} + C_i^m \left| U_i^{*m} \right| U_i^{*m} \tag{21}$$

Einstein's summing rule has not been used in Eq. (21). All variables treated according to Eq. (20) are denoted with an asterisk.

2.3. Turbulence model

In this study, the fabric effect on the turbulence model has been taken into account only with a coarse model.

The near-wall turbulence model of Fluent has been slightly modified.

Naturally, the pore size limits the size of eddies in the fabric. This idea has been used in computing the average distance to the wall in the fabric. It has been computed on the planes that were used for average velocities, according to Eq. (18), where distance to the nearest wall in cell j is assigned to ϕ_j. This quantity has then been treated according to Eq. (20) (assuming that it's value is zero in fabric threads), and the resulting quantity has been used in the two-layer zonal model to replace the distance from a smooth wall, y. Otherwise the model has not been changed.

This model does not take into account, for example, turbulence generation near the fabric threads. The constants in the two-layer zonal model are determined for a boundary layer on a smooth wall. No attempt was made to modify them.

3. Test case

3.1. Determining the resistance of the fabric

A few small-scale simulations were carried out in order to find coefficients C_1, D_1 and C_2, D_2. Coefficients for the third direction were estimated from the values of C_1 and D_1. As the slice thickness h_m was constant, a simple arithmetic average was used.

Measured data for the fabric permeability was provided by the manufacturer. The measurements were made at several pressure differences across the fabric. The data were compared with the cases computed in order to determine C_2 and D_2.

The simulations were carried out with periodic and symmetry boundary conditions on the sides of the fabric unit, and constant pressure levels above and below the fabric. A test case with periodic boundaries on all sides of fabric was also computed. The difference between these cases was negligible. The flow was assumed incompressible and quasisteady, and the realizable k–ε turbulence model of Fluent with the two-layer zonal model, and the first order discretization scheme were used. This rather inaccurate discretization scheme was used because there were some convergence problems with second order discretization scheme, and because it was presumed that much larger error sources existed elsewhere. The mesh size was about 600 000 cells.

The computed and measured permeability values are shown in Fig. 3. The idealistic geometrical model of the fabric causes higher values in the simulations compared to the measurements. It is unlikely that such a large error would be caused only by inaccuracies in the measurements or simulations. The measured resistance has been used in the large-scale model, so that constant values have been assigned to the coefficients C_2 and D_2.

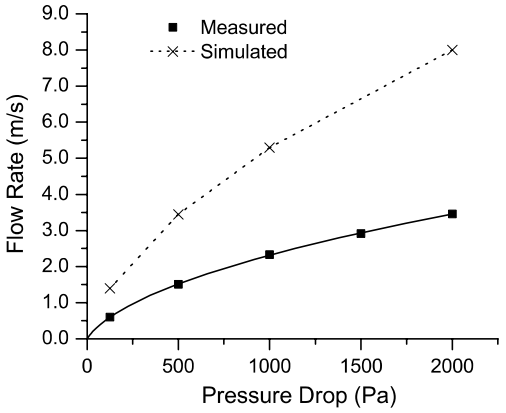

Fig. 3. Measured and simulated permeability of the test fabric in terms of flow rate.

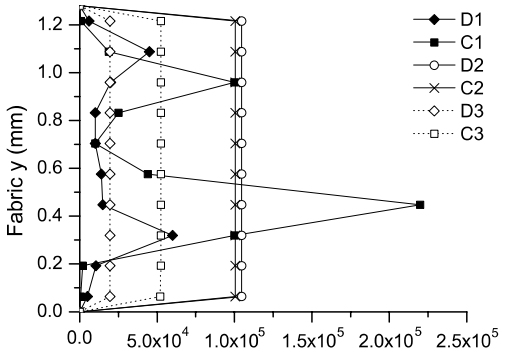

Fig. 4. Fabric model coefficients of the test fabric.

Simulations do not justify this simplification, because simulated results show that most of the pressure loss takes place on the surface of the fabric that first meets the flow. However, the simple model was tested in order to find out initial performance of the model.

The coefficients C_1 and D_1 are very difficult, if not impossible, to determine with measurements. For the test case they were determined by simulations with a pressure inlet boundary condition (total pressure and flow direction specified) for the flow entering the fabric from the side, and pressure outlet (static pressure specified) at the opposite side. Inlet pressures corresponded to free flow velocities 15, 30 and 45 m/s. Periodic conditions in the main flow direction could also be used, but they would not show any effects of non-diagonal forces. Resulting coefficients are shown in Fig. 4.

3.2. Test results

There was experimental data available from wind tunnel measurements, Eriksson (1999), with a pressure difference across the fabric (about 50 Pa) and a velocity component parallel to the fabric (30 m/s). The pressure difference was the highest that could be achieved with

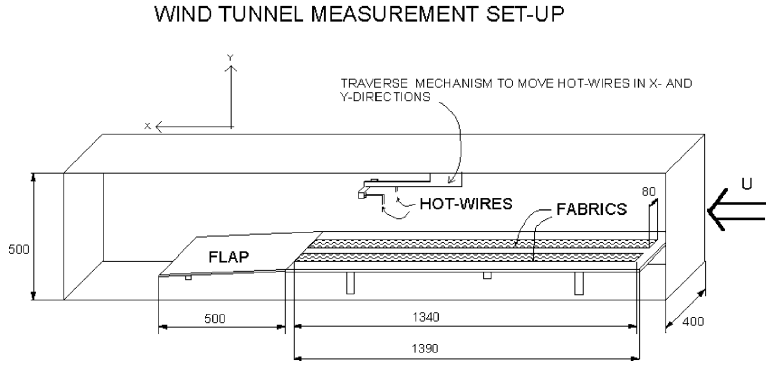

Fig. 5. Wind tunnel measurement set-up (Eriksson, 1999).

the measurement arrangement used. Pressure differences in a paper machine can be much higher, which is why the permeability was originally measured with higher pressure differences by the manufacturer. The measurement arrangement is shown in Fig. 5. The pressure difference was generated by placing a plate (with fabric stripes on it) asymmetrically into the tunnel. Fabric stripes were 80 mm wide and 1340 mm long. There were slots in the plate under the fabric, so that air could flow through the fabric. The slots were 55 mm wide and 1290 mm long.

The measurements (mean and instantaneous velocity components) were carried out on the underpressure side of the fabric. Thus there was blowing to the measured boundary layer, and therefore also a slight negative pressure gradient along the boundary layer (in order of 7 Pa/m in simulations). The measured boundary layer is much thicker than it would be without blowing. With this kind of pressure difference, the boundary layers on the suction side were so thin, that they could not actually be measured. The case described here as an example is only one of the measured ones. The other cases showed consistent model behavior.

The wind tunnel geometry was used in the 3D simulations, so that only half of it was modeled with a symmetry condition in the middle of the tunnel. The mesh consisted of about 2 million cells, and a second order upwind discretization scheme was used. The bars that mounted the plate were not modeled. The boundary layers on vertical sides of the slot in the plate were also not modeled due to mesh size constraints. Instead symmetry conditions were used. The boundary condition for the outflow was a pressure outlet with zero static pressure and a velocity inlet (velocity components specified) for the inflow. The inlet velocity was 30 m/s.

Three cases were tested. In case 1, all proposed models were applied. In case 2, C_1 and D_1 were constants with the same value as C_3 and D_3. In case 3, the turbulence model was omitted. Instead, the fabric zone was defined as laminar, which means that turbulent viscosity and the turbulence generation were set to zero. Coefficients C_1 and D_1 were defined in the same way as in Case 1.

U-velocity profiles at 500 mm from the leading edge of the plate are shown in Figs. 6 and 7. Turbulent kinetic energy profiles at the same position are shown in Fig. 8 and turbulent viscosity profiles at the same position are shown in Fig. 9. Measured turbulent kinetic energy was estimated from $\overline{u'^2}^{0.5}$ and $\overline{v'^2}^{0.5}$ by assuming that $\overline{w'^2}^{0.5}$ is

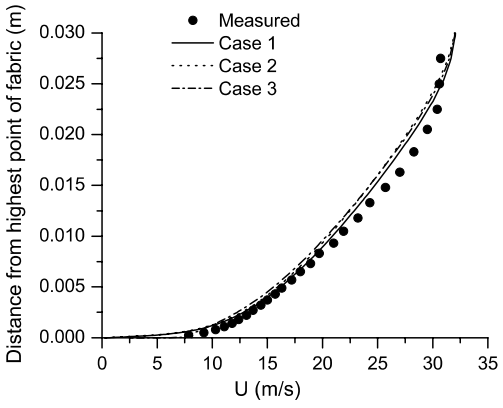

Fig. 6. Velocity parallel to fabric at traverse 500 mm from the leading edge.

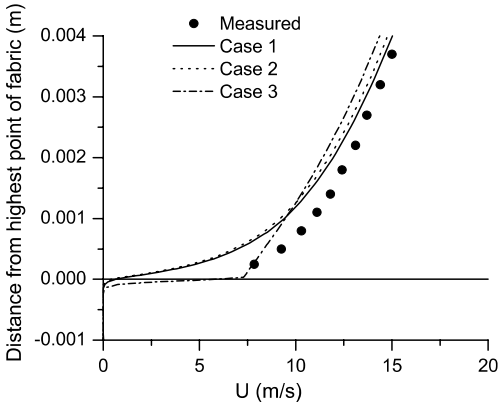

Fig. 7. Initial region of velocity parallel to fabric at traverse 500 mm from the leading edge.

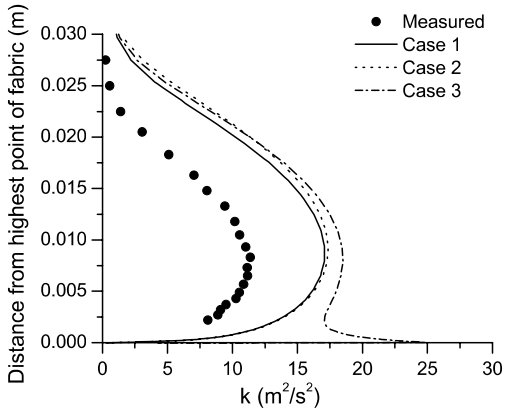

Fig. 8. Turbulent kinetic energy at traverse 500 mm from the leading edge.

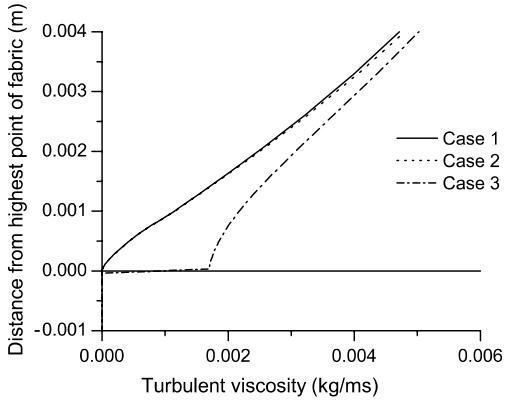

Fig. 9. Turbulent viscosity at traverse 500 mm from the leading edge.

the average of them. Some profiles of $\overline{w'^{2.5}}$ were measured, showing that this assumption is justified. Simulated (case 1) and measured U-velocity profiles at 500 and 880 mm from the leading edge of the plate are shown in Fig. 10.

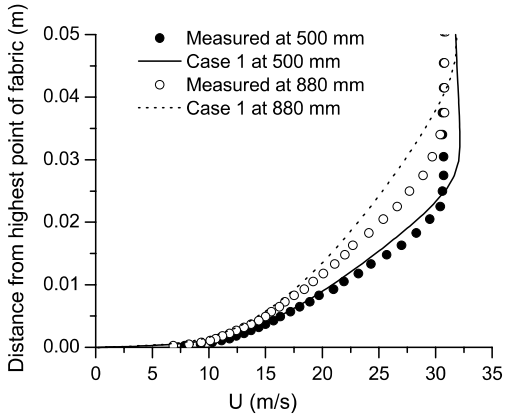

Fig. 10. Velocity parallel to fabric at traverses 500 and 880 mm from the leading edge.

Results show that the velocity profiles for both cases 1 and 2 are rather close to the measured ones, with slightly more accurate results for case 1. As mentioned, the boundary layer on the underpressure side becomes very thick and velocities in the fabric surface small, and therefore the fabric surface modeling has less effect than it would in the case of a thinner boundary layer. Case 3 shows poor results compared to the other two cases. This is caused by the assumption that fabric does not have a direct effect on turbulence in the area outside the fabric. This leads to a non-physical peak value of turbulent kinetic energy in the fabric vicinity. None of the cases matches exactly the measured results. Because the difference between cases 1 and 2 is rather small, it is assumed that this is due to problems in the model of the complete wind tunnel flow and turbulence near the fabric. The velocity boundary condition at the inlet is probably not quite adequate. It enforces a uniform velocity distribution at the inlet, although it is probable that the plate affects the flow at the tunnel opening. Velocities higher than 30 m/s at the edge of the boundary layer are caused by this boundary condition, because a larger amount of air enters the tunnel in the simulations than in the measurements. However, there were no accurate pressure or velocity measurements at the inlet, so the uniform velocity condition was the best available.

Comparison of turbulence values and the corresponding velocity profile very close to fabric surface suggest that turbulent viscosity may be too low in this area in cases 1 and 2. Therefore it is concluded that for better results in the near-fabric area, fabric generated turbulence should be taken into account.

Comparison of the U-velocity profiles at different positions shows that the simulated boundary layer grows faster than the measured one. This can be caused either by the problems in the model of the complete wind tunnel flow, or by turbulence model near the fabric. Fig. 8 shows that all simulated turbulence profiles are rather far from the measured one, and that the difference between different simulation cases is small compared to the difference to the measured profile. This implies that the discrepancy is due to the complete wind tunnel model. There can, for example, be secondary flows that k–ε model cannot predict.

The model according to Eq. (15) gave a smaller transpiration rate through the fabric, and consequently, a thinner boundary layer than measured. However, the simulated pressure difference across the fabric was locally as much as 40 Pa greater than the measured pressure difference. The x-direction coefficients for this model were rederived according to Eq. (15), but the y-direction coefficients were the same as in original model, derived from measurement results. It was concluded that because velocity in the x-direction was zero in the permeability measurements, these coefficients give rise to

greater resistance when a considerable velocity component in the x-direction is present (which is the case especially on the overpressure side of the fabric). This problem is related to the simplification done when assuming constant y-direction coefficients. In order to use the more common definition for inertial resistance, the flow phenomena in the outer layer of the fabric should be more closely studied.

Kuznetsov (2000) has created analytical equations to describe flow on the boundary of porous media and free flow. However, these equations assume uniform porosity and cannot be directly applied to the fabric model proposed.

4. Conclusions

A method for modeling a dryer fabric as a porous media has been proposed. The model includes momentum source terms and turbulence manipulation. The method has been shown to give reasonable results compared to wind tunnel measurements.

The turbulence manipulation near the fabric should be improved. Other improvements include a better way to model the resistance to the flow normal to fabric. Coefficients for this should be a function of flow direction as well, not only position in fabric.

On the other hand, at the present state the model is rather easy to use and stable. As such, it provides a method to analyze how different fabrics affect the flow field in paper machine scales with reasonable accuracy.

Acknowledgements

The author would like to thank Process Flow Ltd. Oy, Metso Inc., Albany Fennofelt Oy and Albany Nordiskafilt and the Technology Development Center of Finland (TEKES) for their financial support of this work.

References

Antonia, R.A., Djenidi, L., 1997. Reynolds stress producing motions in smooth and rough wall boundary layers. In: Advances in Fluid Mechanics. Computational Mechanics Publications, Southampton, pp. 181–199.

Eriksson, P., 1999. The influence of the dynamical permeability on the flow around a rough surface; wind tunnel measurements on dryer fabrics. Internal Report 99/15, Department of Thermo and Fluid Dynamics, Chalmers University of Technology.

Fagerholm, L. Aerodynamical Properties of Dryer Fabrics for High Speed Paper Machines. 1990 Engineering Conference, Tappi Press, pp. 165–174.

Fand, R.M., Kim, B.Y.K., Lam, A.C.C., Phan, R.T., 1987. Resistance to flow of fluids through simple and complex porous media whose matrices are composed of randomly packed spheres. ASME Journal of Fluids Engineering 109, 268–274.

Fluent Incorporated, 1998. Fluent 5 User's Guide. Fluent Incorporated, Lebanon.

Hellsten, A., Laine, S., 1998. Extension of the k–ω-shear-stress transport turbulence model for rough-wall flows. AIAA Journal 36 (9), 1728–1729.

Krogstad, P., 1991. Modification of the Van Driest damping function to include the effects of surface roughness. AIAA Journal 29, 888–894.

Kuznetsov, A.V., 2000. Analytical studies of forced convection in partly porous configurations. In: Vafai, K. (Ed.), Handbook of Porous Media. Marcel Dekker, New York, pp. 269–312.

Laakkonen, K., Kurki, M., Martinsson, L., Toney, M., 2001. CFD Analysis of a Dryer Pocket, 2001 Engineering/Finishing and Converting Conference, Tappi Press.

Mohammadi, P., Pironneau, O., Valentin, F., 1998. Rough boundaries and wall laws. International Journal for Numerical Methods in Fluids 27, 169–177.

Nakayama, A., Kuwahara, F., 1999. A macroscopic turbulence model for flow in a porous medium. ASME Journal of Fluids Engineering 121, 427–433.

Quintard, M., Whitaker, S., 2000. Theoretical analysis of transport in porous media. In: Vafai, K. (Ed.), Handbook of Porous Media. Marcel Dekker, New York, pp. 4–5.